



**HAL**  
open science

## Comparative metabolomics and glycolysis enzyme profiling of embryogenic and nonembryogenic grape cells

Jonathan Parrilla, Cécile Gaillard, Jérémy Verbeke, Mickael Maucourt, Radoslav Aleksandrov, Florence Thibault, Pierrette Fleurat-Lessard, Yves Gibon, Dominique Rolin, Rossitza Atanassova

### ► To cite this version:

Jonathan Parrilla, Cécile Gaillard, Jérémy Verbeke, Mickael Maucourt, Radoslav Aleksandrov, et al.. Comparative metabolomics and glycolysis enzyme profiling of embryogenic and nonembryogenic grape cells. *FEBS Open Bio*, 2018, 8 (5), pp.784 - 798. 10.1002/2211-5463.12415 . hal-01891843

**HAL Id: hal-01891843**

**<https://hal.science/hal-01891843v1>**

Submitted on 26 May 2020

**HAL** is a multi-disciplinary open access archive for the deposit and dissemination of scientific research documents, whether they are published or not. The documents may come from teaching and research institutions in France or abroad, or from public or private research centers.

L'archive ouverte pluridisciplinaire **HAL**, est destinée au dépôt et à la diffusion de documents scientifiques de niveau recherche, publiés ou non, émanant des établissements d'enseignement et de recherche français ou étrangers, des laboratoires publics ou privés.



Distributed under a Creative Commons Attribution 4.0 International License

# Comparative metabolomics and glycolysis enzyme profiling of embryogenic and nonembryogenic grape cells

Jonathan Parrilla<sup>1</sup>, Cécile Gaillard<sup>1</sup>, Jérémy Verbeke<sup>1,2</sup>, Mickaël Maucourt<sup>3,4</sup>, Radoslav A. Aleksandrov<sup>1,5</sup>, Florence Thibault<sup>1</sup>, Pierrette Fleurat-Lessard<sup>1</sup>, Yves Gibon<sup>3,4</sup>, Dominique Rolin<sup>3,4</sup> and Rossitza Atanassova<sup>1</sup>

1 Laboratoire EBI- Ecologie et Biologie des Interactions, Équipe SEVE-Sucres et Échanges Végétaux-Environnement, UMR 7267 Centre National de la Recherche Scientifique, Université de Poitiers, France

2 GReD. UMR CNRS 6293 - INSERM U1103, Université Clermont-Auvergne CRBC, Faculté de médecine, Clermont-Ferrand, France

3 Laboratoire Biologie du Fruit et Pathologie, UMR 1332 Institut National de la Recherche Agronomique, Université de Bordeaux, Villenave d'Ornon, France

4 Plateforme Métabolome du Centre de Génomique Fonctionnelle Bordeaux, MetaboHUB, Institut National de la Recherche Agronomique, Villenave d'Ornon, France

5 Institute of Molecular Biology Bulgarian Academy of Sciences Acad, Sofia, Bulgaria

## Keywords

cell proliferation and cell fate; glycolysis enzyme activities; grape embryogenic and nonembryogenic cells; metabolic behavior

## Correspondence

R. Atanassova, Laboratoire EBI- Ecologie et Biologie des Interactions, Équipe SEVE-Sucres et Échanges Végétaux-Environnement, UMR 7267 Centre National de la Recherche Scientifique, Université de Poitiers, 3, rue Jacques Fort, Bât. B31, TSA 51106 86073 Poitiers CEDEX 9, France  
Fax: 33 (0)5 49 45 41 86  
Tel: 33 (0)5 49 45 41 87  
E-mail: rossitza.atanassova@univ-poitiers.fr

(Received 23 November 2017, revised 6 March 2018, accepted 7 March 2018)

doi:10.1002/2211-5463.12415

A novel biological model was created for the comparison of grapevine embryogenic cells (EC) and nonembryogenic cells (NEC) sharing a common genetic background but distinct phenotypes, when cultured on their respective most appropriate media. Cytological characterization, <sup>1</sup>H-NMR analysis of intracellular metabolites, and glycolytic enzyme activities provided evidence for the marked metabolic differences between EC and NEC. The EC were characterized by a moderate and organized cell proliferation, coupled with a low flux through glycolysis, high capacity of phosphoenolpyruvate carboxylase and glucokinase, and high oxygen consumption. The NEC displayed strong anarchic growth, and their high rate of glycolysis due to the low energetic efficiency of the fermentative metabolism is confirmed by increased enolase capacity and low oxygen consumption.

Many plant species are able to produce new embryos from single somatic cells as a pertinent strategy of asexual reproduction [1]. Such embryogenic cells are a powerful tool for micropropagation and large-scale *in vitro* multiplication of species with limited seed production, germplasm conservation, as well as for genetic transformation of many woody plants, for example, grapevine. To better understand somatic

embryogenesis, it is also important to keep in mind that the zygote is a free cell, whose fate is independent of any surrounding tissue, avoiding neighboring cell communications, and evolving under endosperm nutritional and hormonal signaling. The fact that functional embryos can develop from somatic cells demonstrates that the genetic program for embryogenesis is totally confined within the cell and can function completely in

## Abbreviations

EC, embryogenic cells; NEC, nonembryogenic cells; PCA, principal component analysis; PCV, packed cell volume; TEM, transmission electron microscopy.

the absence of gene products from the maternal environment [2,3]. The similarity between zygotic and somatic embryogenesis is striking and remarkable, considering that somatic embryos develop completely outside of both the physical constraints and the informational context of maternal tissue [4,5]. However, unlike zygotic embryos, the somatic embryos developing *in vitro* need neither desiccation nor dormancy [6,7].

Embryogenic cell (EC) cultures are suspensions of pro-embryogenic masses, which consist of aggregates of small cells [8–12]. Interestingly, the formation of cellular groups is thought to be a prerequisite for maintaining their ability to differentiate into somatic embryos, thereby allowing plant regeneration [13]. Auxins are necessary for preserving the embryogenic character of cells, but they inhibit the induction of somatic embryogenesis [14]. Inversely, the nonembryogenic cells (NEC) do not form embryos in culture, but continue to proliferate as nonorganized cells [15]. Although metabolic studies have been performed on embryogenic and nonembryogenic callus tissue from sugar cane [16,17], the comparisons at cellular level of EC and NEC still remain limited, either to hormonal level [18–21], or to starch synthesis [15] and cell wall components [12].

We performed an in-depth comparison of grape EC and NEC sharing a common genetic background, but cultured on particular nutritional media for maintaining their specific cell fate determination. The comparative analysis of cytological characteristics, growth kinetics, cellular metabolites, and glycolysis enzymes of grape EC and NEC revealed marked differences in their proliferation, metabolic behavior, and glycolytic metabolism.

## Materials and methods

### Plant material

Two grapevine cell suspensions (EC and NEC), both derived from the rootstock hybrid 41B, the most commonly used rootstock in the vineyards of Champagne (a hybrid between *Vitis vinifera* L. cv. Chasselas x *Vitis berlandieri* P.), were used. The EC suspension was subcultured every 2 weeks by transferring 0.3 mL of packed cell volume (PCV) into 25 mL of a half-strength Murashige and Skoog medium, containing glycerol (4.6 g·L<sup>-1</sup>) and maltose (18 g·L<sup>-1</sup>) as carbon sources, as well as naphthoxyacetic acid (NOA) (1 mg·L<sup>-1</sup>) and acid hydrolysate of casein. The NEC suspension was initiated using stem fragments of *in vitro* plants regenerated from the EC and, after its establishment, was subcultured every 2 weeks by transferring 1 mL PCV in 25 mL of fresh Gamborg medium complemented with sucrose (20 g·L<sup>-1</sup>), 1-naphthalene-acetic acid

(NAA) (0.18 mg·L<sup>-1</sup>), and 6-benzylaminopurine (BAP) (1 mg·L<sup>-1</sup>). Both cell suspensions grew under the same controlled physical conditions: constant shaking (110 r.p.m.), in darkness, and at 21 °C.

### Microscopy

The samples were fixed in 2% paraformaldehyde/0.5% glutaraldehyde with 0.1M Sörensen buffer pH 7.3, for 45 min, at 24 °C. After washing in the same buffer supplemented with 7.5% sucrose, the postfixation in 1% osmium tetroxide was performed for 5 min. The dehydrated samples were embedded in London Resin White and incubated 24 h at 60 °C for polymerization. Sections were obtained using EMUC6 Leica Microtome. Periodic acid/Schiff (PAS) reaction was used for starch visualization on semi-thin sections (500 nm) fixed on polylysinated (1 mg·mL<sup>-1</sup>; w/v) slides. For transmission electron microscopy (TEM) on Jeol JEM 1010 microscope at 80 kV, the ultra-thin sections (60 nm) were collected on gold grids and stained with uranyl acetate and lead citrate.

### Growth kinetics and cyclin gene expression

Cells were filtered, weighted for growth curves, and frozen in liquid nitrogen every 2 days within the 2 weeks time of culture. RNA was extracted using the Spectrum™ Plant Total RNA Kit (SIGMA-Aldrich, Saint-Quentin Fallavier, France) and retrotranscribed with M-MLV retrotranscriptase (Promega, Charbonnières-les Bains, France) following the respective manufacturers' instructions. Cyclins' expression was then determined by qRT/PCR (Promega qPCR Master Mix, Mastercycler realplex<sup>2</sup>). Four housekeeping genes have initially been tested: two elongation factors (VvEF1a, VvEF1 g), actin (VvACT1) and glyceraldehyde-3-phosphate dehydrogenase (VvGAPDH). Of all these, actin was the most stable and therefore chosen as a reference in our cellular models. The cyclin expression was normalized toward the actin as reference gene, using the 2<sup>-ΔCt</sup> method and the following respective primers:

*VvCycA2;2* (XM\_010650250.1)

F 5'-CATGTTGCCAGGTCGATGTAAC-3'; R 5'-GAATGGCTCTGACATCATAACAAC-3'

*VvCycD3;3* (XM\_002285284.3)

F 5'-GGCTGGCATTTCGAAACAGAAAGG-3'; R 5'-GGGAAGTGGGAAGTGGGAAGAGAC-3'

*VvActin* (XM\_002282480.3)

F (5'-GCATCCCTCAGCACCTTCCA-3'; R 5'-AACCC-CACCTCAACACATCTCC-3'.

### Metabolomic analysis

For the <sup>1</sup>H-NMR analysis, polar metabolites were extracted, titrated, lyophilized (EZ Dry-FTS system),

solubilized, and pretreated as described by Moing *et al.* [22].  $^1\text{H-NMR}$  spectra were recorded at 500.16 MHz and 300K on a Bruker Avance III spectrometer using a 5 mm inverse probe and an electronic reference for quantification (Digital ERETIC, Bruker TopSpin 3.0). The assignments of metabolites in the NMR spectra were made by comparing the proton chemical shifts with literature values [23–25], with the spectra of authentic compounds recorded under the same buffer conditions and by spiking the samples with standards. Metabolite concentrations in the NMR tube were calculated using Analytical Profiler mode of AMIX software (version 3.9.10, Bruker) for calculation of resonance areas, followed by data export to Excel software. 2D-homonuclear correlation spectroscopy ( $^1\text{H-}^1\text{H}$  COSY) experiments were carried out to verify the identity of known compounds and to check whether unknown signals really correspond to different compounds. Starch was determined as described in Hendriks *et al.* [26].

### Oxygen consumption

The consumption of oxygen ( $\text{O}_2$ ) by both types of cells is measured using the Clark electrode (DUAL DIGITAL MODEL 20, RANK BROTHERS LTD). The rate of oxygen consumption was followed during 20 min on 20 mg cells maintained in the dark and was estimated in  $\text{nmols O}_2 \cdot \text{min}^{-1} \cdot \text{g}^{-1}$  dry weight [27].

### Enzyme activities

Extraction was performed as described by Nunes-Nesi *et al.* [28]. All enzyme activities were carried out on a robotized platform [29] and assayed as described, respectively: phosphoglucose isomerase—PGI [30]; enolase and triose-phosphate isomerase—TPI [31]; phosphoglucomutase—PGM [32]; pyruvate kinase—PK, glucokinase—GK, fructokinase—FK, phosphoenolpyruvate carboxylase—PEPC and ATP-dependent phosphofructokinase—PFK [29]; phosphoglycerokinase—PGK [33]; aldolase [34].

## Results

### Cytological characterization

The cytological study of both cell types harvested during the growth phase revealed important differences (Fig. 1). The EC clusters displayed an apparent homogeneity mimicking sand grains, composed of distinct groups of many small cells (10 to 20  $\mu\text{m}$  wide) surrounded by a kind of thin gel coat (Fig. 1A). Inversely, the NEC were larger in size (50 to 60  $\mu\text{m}$  in size) and formed very small groups of several adjacent cells (Fig. 1B). The nucleo-cytoplasmic ratio of EC was significantly higher ( $0.60 \pm 0.09$ ) compared to that of the

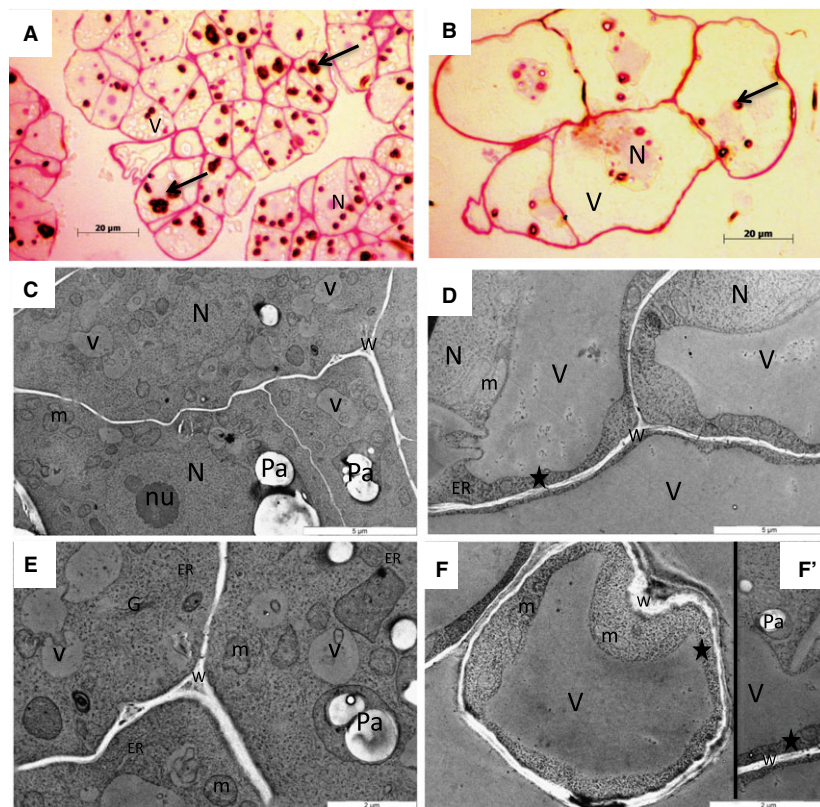


**Fig. 1.** Microscopy observation of grape EC and NEC. Photonic microscopy: A. Clusters of numerous and small-sized EC, with the nuclei (N) in the central part, small vacuoles (v) and many amyloplasts (arrow); B. small groups of large NEC with the nuclei at the cell periphery, one or two large vacuoles (V) and some amyloplasts (arrow). Transmission microscopy: C and E. In EC: many small vacuoles (v) in the dense cytoplasm, large starch grains in amyloplasts (Pa), many mitochondria (m), long profiles of endoplasmic reticulum (er), and Golgi stacks (G); D, F, and F'. In NEC: thin layer of cytoplasm (asterisk) adjacent to the cell wall (W), long mitochondria profiles, amyloplasts with small starch grains, short profiles of endoplasmic reticulum PFA/glutaraldehyde/OsO<sub>4</sub>/LRW. A and B. PAS staining—starch grains were purple-stained and cell walls pink-stained; C-F'. uranyl/lead contrast—starch grains were white-stained because of their high optic density.

NEC ( $0.44 \pm 0.10$ ). The nuclei of EC were localized in the cell center, while the nuclei of NEC were usually at the cell periphery. The vacuolar apparatus of EC was composed of several small vacuoles (1 to 2  $\mu\text{m}$ ) embedded in a dense cytoplasmic matrix (Fig. 1C,E). The NEC presented one or two large vacuole(s), reaching 20 to 40  $\mu\text{m}$ , compressing the cytoplasm as a thin layer to the cell wall (Fig. 1D,F). The EC presented a lot of large starch grains in amyloplasts 1 to 3  $\mu\text{m}$  wide (mean  $2.26 \pm 0.94$ ) (Fig. 1A,C, and E), while the NEC contained smaller amyloplasts (mean  $1.17 \pm 0.26$ ) without any important starch reserves (Fig. 1B, D,F, and F'). In EC, abundant and small-sized mitochondria (0.5 to 1  $\mu\text{m}$  in width) with dense matrix and large cristae occurred together with many ribosomes forming polysomes, Golgi stacks, and a large amount of long endoplasmic reticulum profiles of rough-type. By contrast, NEC mitochondria were often elongated (2  $\mu\text{m}$  long and 1  $\mu\text{m}$  large) with large electron lucent cristae and the endoplasmic reticulum had very short profiles.

### Proliferation characteristics

The different proliferation behavior of both cell types was reflected by their distinct growth curves, obtained through the fresh mass (Fig. 2A,B). The EC were characterized by slow and progressive proliferation, revealing their aptitude to grow for at least 1 month on the same culture medium without an apparent stationary phase (Fig. 2A). By contrast, the NEC displayed three phases: latent (from 0 to 2 day), growth (from 2 to 8 day), and stationary (from 10 to 14 day), and their survival was strongly dependent on subculture in a fresh nutritional medium (Fig. 2B).

In this regard, the RT/qPCR analysis of two genes encoding cyclins *VvCycD3;3* and *VvCycA2;2* surprisingly demonstrated a higher level of expression in EC (Fig. 2C,D) compared to that of NEC (Fig. 2E,F). At day 2 after subculture, EC presented a twofold initial increase in cyclin gene expression that reached a maximum at days 4 and 6 and at days 6 and 8, respectively, for *VvCycD3;3* and *VvCycA2;2*. After day 8, their

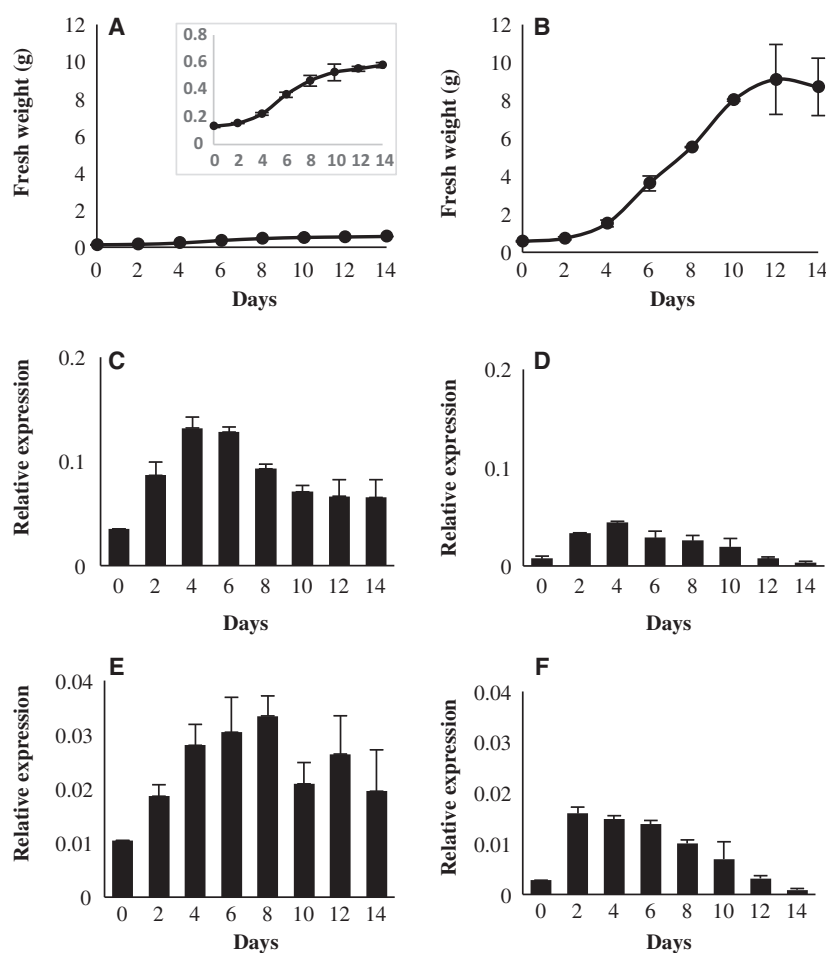


**Fig. 2.** Growth curves of grape EC (A) and NEC (B) obtained using the fresh weight of filtered cells at each time point during the culture period (mean values from three independent biological replicates). Expression profiles of *CycD3;3* (C and D) and *CycA2;2* (E and F) genes, respectively, in EC (C and E) and NEC (D and F) (mean values from three biological replicates).

expression remained stable at a level similar to that at day 4. An at least threefold more important expression of *VvCycD3;3* was observed, when compared to that of *VvCycA2;2*. Conversely, NEC demonstrated a lower level and a transient pattern of expression induction for both cyclins. At day 2, they displayed an initial fivefold to sixfold induction, respectively, for *VvCycD3;3* and *VvCycA2;2*, with a maximum at day 4, followed by a relatively stable level during the growth phase, and a critical drop before to reach the initial expression level at day 14.

### Comparison of the intracellular metabolites

The intracellular metabolite comparison of the EC and NEC was achieved by quantitative proton NMR analysis at seven time points during the 14 days of culture. We quantified six soluble sugars (glucose, fructose, maltose, sucrose, galactose, and fucose), two alcohol sugars (glycerol and inositol), seven organic acids (acetate, fumarate, citrate, succinate, formate, galacturonate, and malate), 15 amino acids (alanine, asparagine, aspartate, gamma amino butyric acid, glutamine, glutamate, isoleucine, leucine, histidine, phenylalanine, serine, tryptophan, valine, proline, and tyrosine), and two polyamines (cadaverine and putrescine) in the two cell types. In total,  $^1\text{H}$  NMR enabled the detection of 42 metabolites, from which 36 could be identified. This result was in line with the previously described detection capacity of the chosen method [35].

Principal component analysis (PCA) was used to visualize the discriminating differences between both cell types (Fig. 3A). The first PCA axis, corresponding to 42.02% of the variance, revealed the spectacular cleavage between EC and NEC. The EC were perfectly clustered throughout the subculture period, displaying a high level of homogeneity. They were characterized by low levels of both maltose and glucose and by high levels of glycerol, alanine, proline, and some compounds related to the B group vitamins—choline and trigonelline, as detailed in Fig. 3B.

The NEC displayed two internal groups reflecting a changing metabolite profile during the subculture period (Fig. 3A,B). The evidence for this particularity was provided by the second PCA axis responsible for 32.72% of the variance (Fig. 3A). The first group of NEC corresponded to the latent and growth phases from day 0 to day 10, while the second corresponded to the establishment of the stationary phase (days 12 and 14). The NEC in proliferation presented high concentrations of soluble sugars (sucrose and glucose) and organic acids (citrate, fumarate, succinate, malate) (Fig. 3B).

The second axis was positively correlated with the intracellular concentration of some amino acids (aspartate, valine, asparagine, leucine, tryptophan, histidine, and phenylalanine) and the polyamine cadaverine. The concentration of free amino acids sharply increased at days 12 and 14 in the NEC, suggesting an induction of proteolysis at the stationary phase. The appearance of

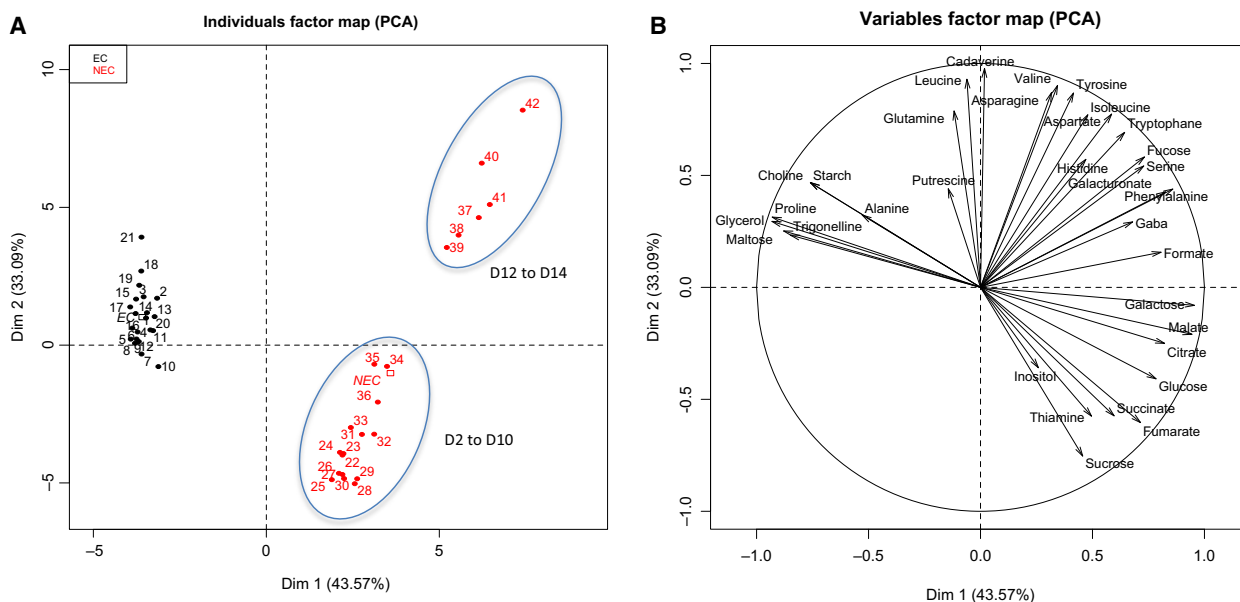


**Fig. 3.**  $^1\text{H}$ -NMR analysis of intracellular soluble metabolites (sugars, amino acids, organic acids, etc.) throughout the growth kinetics of both cell cultures. Principal component analysis (PCA) by individual factor map (A) and variable factor map (B) of EC (black) and NEC (red). The numbers correspond to a total of 42 samples (three biological replicates for the seven time points of harvest during fourteen days of subculture for each of both cell types). Starch content was enzymatically determined.

fucose, a deoxyhexose largely involved as the terminal sugar of protein N-glycosylation, also confirmed this possibility. Another fact arguing in favor of the enhanced cell death at this latter phase concerned the accumulation of galacturonic acid and fucose, as valuable indicators of cell wall degradation.

A quantitative comparison of identified cellular metabolites, performed by  $^1\text{H-NMR}$  analysis of both cell types during 14 days of the subculture period, is presented in detail in Fig. 4 and S1. Despite the relatively similar concentrations of sucrose and glucose in the NEC, fructose was only detected at day 2 and its level was approximately one-third that of glucose. Throughout this subculture period, starch concentration in the EC was higher than that in the NEC. In the EC, the starch content remained stable during 14 days, while in the NEC, it dropped down at the stationary phase. Two other compounds considered as compatible osmolytes, the amino acid proline and the amino alcohol choline (a quaternary ammonium), displayed relatively stable concentrations all over the proliferation of EC, but they were almost undetectable in the NEC. The total protein content of EC at day 8 was four times higher than these of NEC. The unique metabolite presenting the same very constant concentration for both cell types was inositol, an important source of key second messengers for the intracellular hormonal signaling.

### Comparison of culture medium metabolites

In complement to the intracellular metabolites, a metabolic profiling  $^1\text{H NMR}$  study of the culture media was carried out. PCA was performed using all compiled data that were obtained throughout cell proliferation. As shown in Fig. 5, the first axis displays 75.93% of variance, which highlights the strong discrimination of the media used to culture EC and NEC. As both cell types were cultured on two distinct nutritional media, the comparison of extracellular metabolites allowed a better understanding of their nutritional behavior. Once again, the metabolites of the EC medium were perfectly matching and form a unique homogenous group (Fig. 5A). As expected, the culture medium of EC was characterized by high content of maltose, glycerol, and amino acids during the growth phase (Fig. 5B). Inversely, the metabolites of the NEC medium manifested two separate groups, corresponding, respectively, to the first part of the growing curve (days 0-6) and to the second part (days 8-14) (Fig. 5A). Elevated concentrations of sucrose, glucose, and fructose predominated between day 0 and day 6, while acetate, ethanol, and glucuronate accumulated mainly between days 8 and 14 (Fig. 5B).

The detailed analysis of all detected compounds in the culture media was presented in Figs 6 and S2. In EC, the carbon sources maltose and glycerol were used with parsimony throughout the 14-day period, as additionally confirmed by the very low and relatively stable level of glucose. A second specific characteristic consisted in the maintaining of a very stable level of amino acids concentration during the subculture period, apparently due to the presence of casein hydrolysate, but also revealing a relatively low consumption by EC.

In the culture medium of NEC, the three soluble sugars (i.e., sucrose and its cleavage products glucose and fructose) were detected. Sucrose concentration displayed a rapid early decline, during the cell growth phase, and a complete depletion at day 8. This phenomenon was possibly due to loosely bound parietal invertases, which efficiently hydrolyze sucrose in culture medium. Between the two products of sucrose cleavage, glucose appeared as the preferred substrate of hexose transporters and sugar metabolism, as it was undetectable from day 8, while fructose was still measurable at day 10. The fact that ethanol, acetate, and formic acid accumulated over time in the culture medium revealed that anaerobic metabolism (fermentation) was taking place in these cells.

### Oxygen content as evidence for cell metabolic activity

To obtain an appropriate estimation for the level of the oxidative phosphorylation in EC and NEC, oxygen consumption was measured with an oxygen electrode. The chosen time points corresponded to each of the three phases of proliferation, that is, latent (days 0-2), growth (days 2-8), and stationary (days 10-14). The oxygen content was normalized to the dry weight of cells, thus minimizing the cell size differences. Despite a certain decline of the oxygen level in EC at day 8, the rate of electron flow to oxygen remained relatively stable for both cell types and especially for the NEC. The most striking observation consisted in the fact that the EC consumed twice as much oxygen as the NEC (Fig. 7).

### Profiling of enzyme activities in the glycolysis pathway

The profiles of the capacities (i.e., activities measured under substrate saturating conditions) of the glycolysis enzymes measured at day 8 were very different between the two types of cells (Fig. 8A,B,C,D). The twelve measured enzymes could be clustered in three categories based on their activities, which ranged from 2000 to 200 000  $\text{nmol}\cdot\text{g}^{-1}\text{DW}\cdot\text{min}^{-1}$ . Both cell types



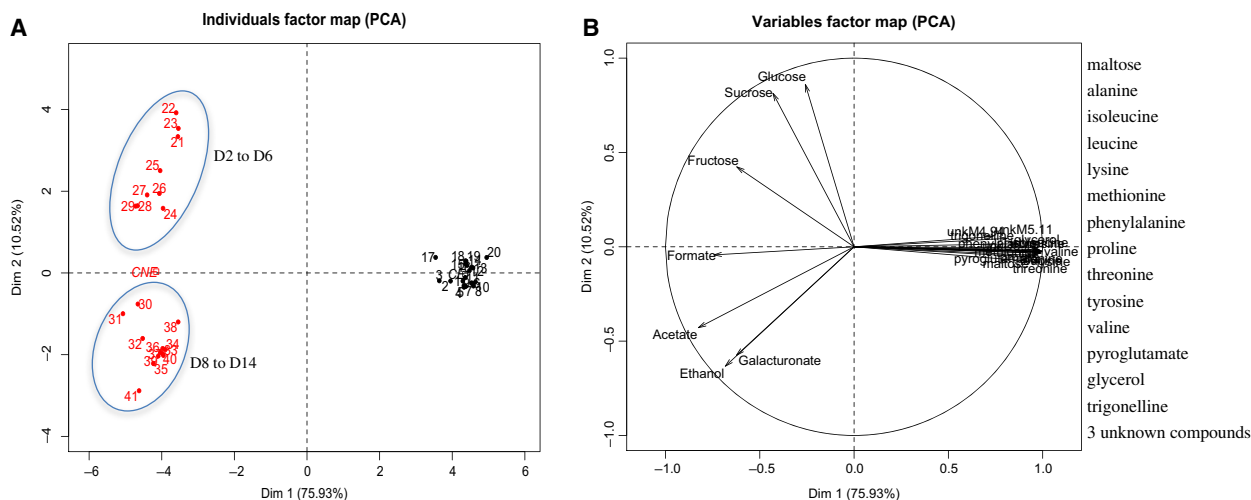


**Fig. 5.**  $^1\text{H}$  NMR analysis of the soluble metabolites of both cell culture media (sugars, amino acids, organic acids, etc.) throughout the growth kinetics of both cell cultures. Principal component analysis (PCA) by individual factor map (A) and variable factor map (B) of EC (black) and NEC (red). The numbers correspond to a total of 42 samples (three biological replicates for the seven time points of harvest during fourteen days of subculture, for each of both cell types).

were characterized by enzymes of the irreversible steps of glucose metabolism (glucokinase, fructokinase, phosphofructokinase) with high capacities (Fig. 8B). The EC displayed higher capacities of enzymes catalyzing the reversible reactions in the upper part of glycolysis (phosphoglucose isomerase, aldolase, triose-phosphate isomerase, phosphoglucomutase, phosphoglycerokinase) as well as phosphoenolpyruvate carboxylase and pyruvate kinase, which are both situated at the lower part of glycolysis and use phosphoenolpyruvate as substrate (Fig. 8C,D). Inversely, the NEC were characterized by an important enolase activity and by very low phosphoenolpyruvate carboxylase and pyruvate kinase activities (Fig. 8C).

## Discussion

The main challenge of the present study was to compare the metabolic behavior of EC and NEC sharing a common genotype but evolving as two independent phenotypes maintained on their most appropriate culture media. It should be stressed that none of the cell types can maintain its phenotype and specific cell fate determination in the opposite medium.

### Cytological characteristics and proliferation specificities

The EC characteristics, dense cytoplasm, small vacuoles, high nucleo-cytoplasmic ratio, numerous polyosomes, active mitochondria, ER, and Golgi (Fig. 1A,

C, and E) argue in favor of a cell division coupled with cytoplasmic growth, which implies the accumulation of macromolecules and cellular components, as described for meristematic cells [36,37]. Conversely, the NEC displayed one or two large vacuole(s), a small nucleo-cytoplasmic ratio, electron lucent cristae, and small endoplasmic reticulum profiles (Fig. 1B,D,F, and F'), features coupling the cell division to the cell expansion growth [37].

The expression profiles of the cyclin genes, *VvCYCD3;3* and *VvCYCA2;2*, also demonstrated the differences in cell division activity of EC and NEC (Fig. 2C,D,E, and F). The choice of these two distinct types of cyclins shed light on two crucial transitions between the phases of cell cycle, the G1/S and the G2/M, respectively [38]. The *VvCYCD3;3* gene belongs to the D-type cyclins known to display a certain functional redundancy required for normal embryonic development [39]. The expression of *CYCD3* genes has been demonstrated as regulated at transcriptional level by cytokinins, and this hormonal control is efficiently mimicked by sucrose, which also acts as a metabolic signal [40,41]. Thus, the presence of cytokinins and sucrose in fresh culture medium may explain the sharp induction of *VvCYCD3;3* after the subculture of NEC. Inversely, the decrease in cyclin gene expression at the stationary phase due to the sucrose depletion argues in favor of a strong but anarchic proliferation of NEC. As sucrose availability is crucial for commitment to plant cell division during G1 phase by controlling the expression of D-type cyclins [42], a plausible explanation for the

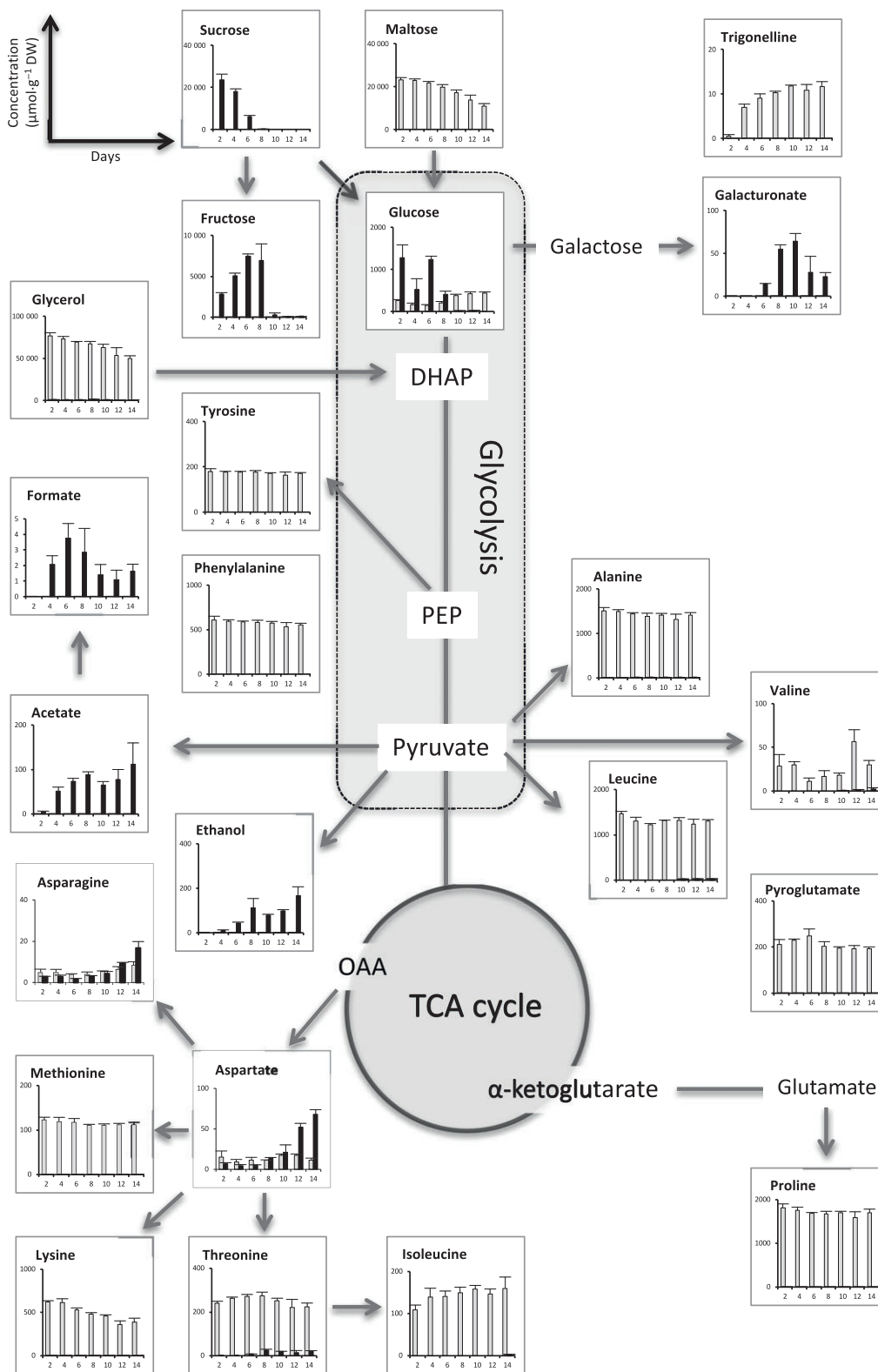


**Fig. 6.** Quantitative comparison of the metabolites in culture medium of each cell type related to glycolysis pathway and TCA cycle (mean values from three biological replicates): EC (columns in gray) and NEC (columns in black).

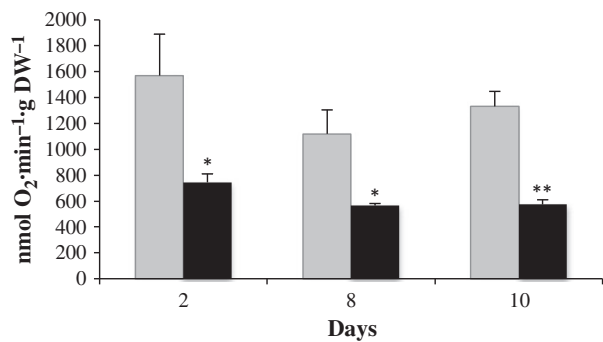


**Fig. 7.** Rate of oxygen consumption throughout cell growth: day 2 (latent phase), day 8 (growth phase), and day 10 (stationary phase); EC (columns in gray) and NEC (columns in black). The results of Kruskal–Wallis test are presented as follows: \**P* value < 0.05; \*\**P* value < 0.01.

strong expression of *VvCYCD3;3* in EC may consist in their partial synchronization in G1 phase due to the sucrose starvation. The sustained expression of both cyclin genes provides evidence for a moderate but organized proliferation of the EC throughout the subculture period, assumption supported by the specific profiles of expression of many cell-cycle genes in synchronized cell cultures of *Arabidopsis* [43,44].

In *Arabidopsis* seeds during the embryo development, the enhanced cell proliferation has been associated with the increased expression of D3- and B1-type cyclins in *megaintegumental/auxin response factor 2* (*mnt/arf2*) and *apetala 2* (*ap2*) mutants, affected in the corresponding transcription factors responsible for the downregulation of these cyclins [45,46]. The triple *Arabidopsis* mutant *cyd3;1/2/3* is characterized by a

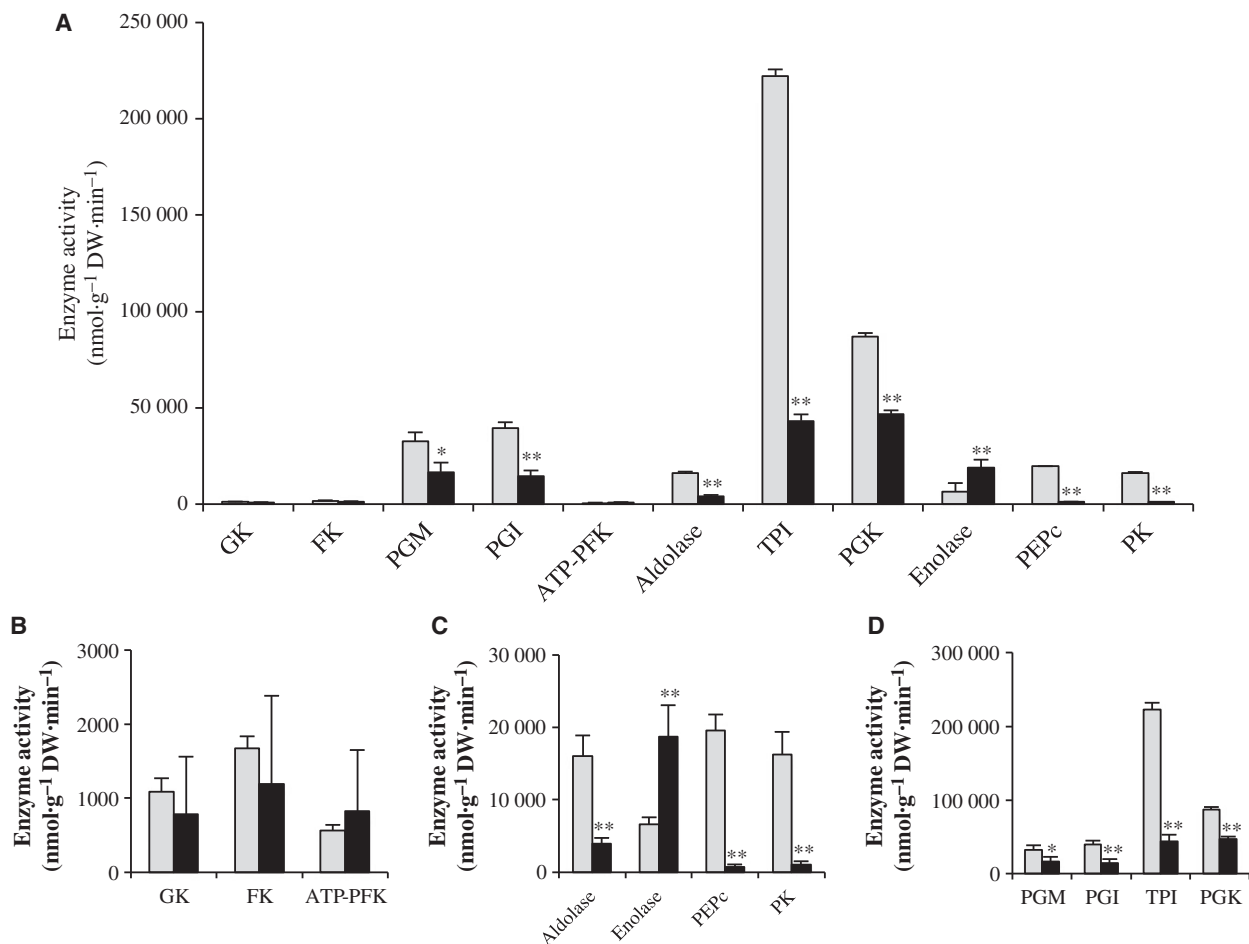


**Fig. 8.** Activity of the glycolysis pathway enzymes: GK—glucokinase, FK—fructokinase, PGM—phosphoglucomutase, PGI—phosphoglucose isomerase, PFK—phosphofructokinase, aldolase, TPI—triose-phosphate isomerase, PGK—phosphoglycerokinase, enolase, PEPC—phosphoenolpyruvate carboxylase, PK—pyruvate kinase. A. The activity of all studied enzymes is presented at the same scale. For a better visualization, B, C, and D present the maximum capacity of each from three groups of enzymes with comparable levels: EC (columns in gray) and NEC (columns in black). The results of Kruskal–Wallis test are presented as follows: \**P* value < 0.05; \*\**P* value < 0.01.

reduction in cell number compensated by an increase in cell size and DNA content [47]. Furthermore, it has been demonstrated that transcripts of *CYCA* genes, such as *CYCA2;1* and *CYCA2;3*, accumulate at the G2 to M transition in a manner concomitant with these of all *CYCB* genes. The fact that *CYCA2;1* expression is related to cell division was further confirmed by the promotion of the endoreduplication by its proper mutation [48].

### Metabolic behavior and profiling of glycolysis enzyme activities

The detailed <sup>1</sup>H-NMR analysis of intracellular metabolites emphasized some marked metabolic discrepancies between EC and NEC summarized in Fig. 9. It appears that EC are able to maintain a low intracellular content of glucose and sucrose, in parallel with the synthesis and storage of starch, amino acids (in particular proline and alanine), choline, and proteins. Considering the fact that EC have a relatively low but maintained division activity, the influx of maltose coupled with a less efficient glycolysis (glycerol effect) may explain the starch accumulation in numerous amyloplasts. Inversely, NEC demonstrated a high intracellular level of glucose and sucrose, as well as of some TCA cycle intermediates (citrate, succinate, fumarate, malate).

Although sucrose is the classical sugar in cell suspensions, the use of maltose in embryogenic cell culture and the subsequent induction of somatic embryogenesis are now largely applied for numerous plant species [36,49–52]. The most credible reason for understanding the beneficial effect of maltose on somatic embryogenesis consists in the low hydrolysis of this disaccharide by the extracellular  $\alpha$ -glucosidase, which has been at least five times slower than the sucrose hydrolysis by the cell wall invertases in barley microspore culture [53]. The assimilation of supplied carbon from [<sup>14</sup>C]sucrose has been demonstrated to be remarkably greater than that from [<sup>14</sup>C]maltose. In addition, the authors provided evidence that the adenylate energy charge (ATP and ADP) increased, when the microspores were transferred to maltose, and, inversely, it decreased after transfer to sucrose at the same concentration (40 mM).

Contrary to most yeast species relying on glycerol as a carbon substrate in aerobic conditions, plant cells do not use it efficiently as a growth substrate. For example, in mesophyll cells from barley leaves, glycerol triggers an accumulation of glycerol-3-phosphate at the expense of intracellular Pi and impairs phosphate metabolism and photosynthesis [54]. The growth of excised

maize root tips is also inhibited in the presence of 100 mM glycerol [55]. Glycerol, which may provide carbon to the glycolysis via a phosphorylation (glycerokinase) followed by an oxidation (glycerol-3-phosphate dehydrogenase), is not only a poor substrate for plant cell growth, but also a disturbing factor, which slows down the glycolysis flux. This is consistent with the known inhibition of glucose-6-phosphate isomerase by glycerol-3-phosphate [56]. Two independent analyses realized on citrus and chicory cells cultured on medium containing glycerol as only carbon source have demonstrated the synthesis of soluble sugars (sucrose, glucose, fructose) as well as of starch [57,58]. These latter observations are in agreement with the starch accumulation in grape EC and argue in favor of a possible role of glycerol in the stimulation of gluconeogenesis.

It is very likely that NEC strongly rely on fermentative metabolism to generate ATP, as fermentation products ethanol and formic acid were found in the culture medium (Fig. 6), and enolase activity was very high compared to EC (Fig. 8). It is striking that high enolase characterizes a range of cancer cells but also yeast [59], which both use the Warburg effect to increase their cell proliferation rate under favorable conditions (for instance high sugar supply). The partial switch of NEC to fermentation was corroborated by their more rapid cell growth (Fig. 2A,B) and confirmed by their two times lower oxygen consumption rate (Fig. 7) than those of the EC. Moreover, due to low energy efficiency, fermentative metabolism requires a high metabolic flux through glycolysis. Inversely, phosphoenolpyruvate carboxylase and pyruvate kinase activities were much higher in EC compared to NEC (Fig. 8). One explanation could be that in EC, these activities need to be relatively high to support the supply of carbon into the TCA cycle, and thus, the synthesis of ATP and carbon skeletons to cell growth.

### Cross-talk of hormonal and metabolic regulation

In cells displaying embryogenic potential but maintained on noninducing medium, auxin depletion induces the synthesis of  $\alpha$ -amylases and the stimulation of starch catabolism [60]. The same authors have demonstrated the importance of metabolic regulation, namely the fact that the decrease in soluble sugars level may produce the same derepression effect on the genes encoding starch degradation enzymes. The already-described opposite effects of auxins and cytokinins on amyloplast development and starch synthesis genes in the BY2 tobacco cells [61], coupled to the quick sucrose metabolism fueling the high rate of cell

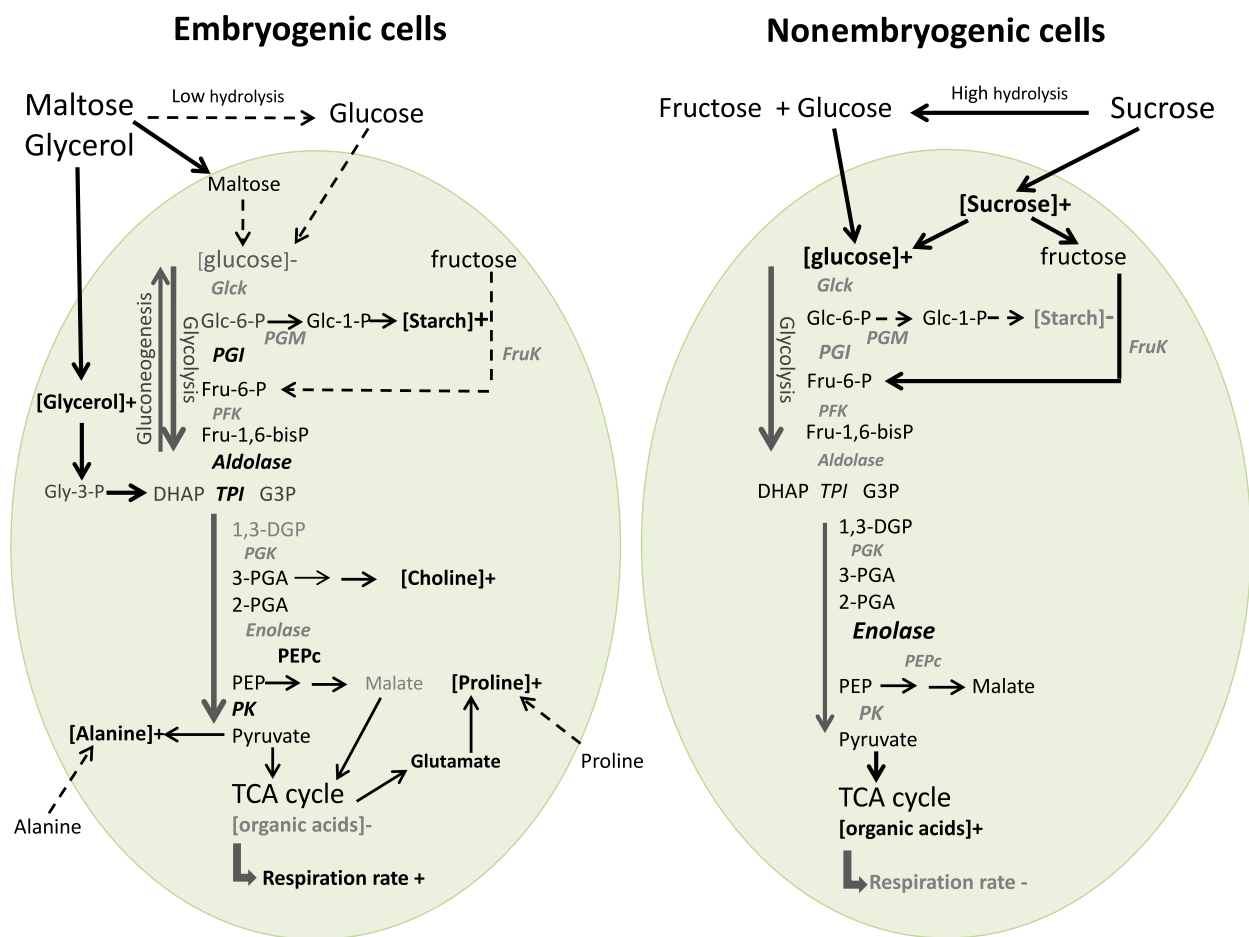


**Fig. 9.** Schematic presentation summarizing the main differences in glycolysis pathway efficiency of grape EC and NEC. Enzyme abbreviations: GK—glucokinase, FK—fructokinase, PGM—phosphoglucumutase, PGI—phosphoglucose isomerase, PFK—phosphofruktokinase, TPI—triose-phosphate isomerase, PGK—phosphoglycerokinase, PEPC—phosphoenolpyruvate carboxylase, PK—pyruvate kinase. The names and the arrows in bold correspond to higher enzyme activities and metabolite fluxes than those in normal font and dashed lines.

division, are therefore arguments in favor of the low starch content in NEC. Inversely, the EC are cultured at the conditions of high auxin repression of starch degradation. Their ability to maintain a low cellular level of glucose may be due to the maltose and the glycerol as carbon sources, which impose a low glycolysis flux at the expense of starch accumulation. Our model is a pertinent example that the low glycolysis flux is required to prevent the EC from differentiating. The low glycolytic metabolism under high auxin pressure thereby hinders the differentiation of the EC through somatic embryogenesis.

### Conclusion

Our results fill in the literature gap by providing evidence for the marked metabolic differences between

EC and NEC. These new data highlight the NEC as a model of strong and anarchic cell proliferation, while the EC as a model of cell ability to switch from moderate and organized cell proliferation toward differentiation. These both cell types with differential efficiency of glycolytic metabolism and distinct cell fate open perspectives for the study of gene expression regulation in the glucose signaling pathways, at the cross-talk of hormonal and metabolic signals.

### Author contributions

RA, JP, DR, YG, and PF designed the experiments. JP, CG, JV, MM, RAA, and FT performed the experiments. RA, JP, DR, YG, and PF discussed the data. RA wrote the manuscript. RA, DR, and YG revised the article. All authors approved the final manuscript.

## Funding

This work was supported by the National Center of Scientific Research, the University of Poitiers, the Poitou-Charentes Region (PhD grant of JP), the ERASMUS student program (Master's degree grant to RAA), the Metabolome Platform of Functional Genomics Center of Bordeaux-MetaboHUB, the National Institute of Agricultural Research Bordeaux-Center, the State-Region Planning Contracts (CPER), and the European Regional Development Funds (FEDER).

## Conflict of interest

The authors declare that the research was conducted in the absence of any commercial or financial relationships that could be considered as a potential conflict of interest.

## References

- Vogel G (2005) How does a single somatic cell become a whole plant? *Science* **309**, 86.
- Verdeil JL, Alemanno L, Niemenak N and Tranbarger TJ (2007) Pluripotent versus totipotent plant stem cells: dependence versus autonomy? *Trends Plant Sci* **12**, 245–252.
- Ikeuchi M, Iwase A, Rymen B, Harashima H, Shibata M, Ohnuma M, Breuer C, Morao AK, De Lucas M, De Veylder L *et al.* (2015) PRC2 represses dedifferentiation of mature somatic cells in Arabidopsis. *Nat Plants* **1**, 15089.
- Zimmerman JL (1993) Somatic embryogenesis: a model for early development in higher plants. *Plant Cell* **5**, 1411–1423.
- Guan Y, Li S-G, Fan X-F and Su Z-H (2016) Application of somatic embryogenesis in woody plants. *Front Plant Sci* **7**, 938.
- Dodeman VL, Ducreux G and Kreis M (1997) Zygotic embryogenesis versus somatic embryogenesis. *J Exp Bot* **48**, 1493–1509.
- Fehér A (2015) Somatic embryogenesis - Stress-induced remodeling of plant cell fate. *Biochim Biophys Acta* **1849**, 385–402.
- Verdeil JL, Hocher V, Huet C, Grosdemange F, Escoute J, Ferrière N and Nicole M (2001) Ultrastructural changes in coconut calli associated with the acquisition of embryogenic competence. *Ann Bot* **88**, 9–18.
- Namasivayam P, Skepper J and Hanke D (2006) Identification of a potential structural marker for embryogenic competency in the Brassica napus spp. oleifera embryogenic tissue. *Plant Cell Rep* **25**, 887–895.
- Shang H-H, Liu C-L, Zhang C-J, Li F-L, Hong W-D and Li F-G (2009) Histological and ultrastructural observation reveals significant cellular differences between Agrobacterium transformed embryogenic and non-embryogenic calli of cotton. *J Integr Plant Biol* **51**, 456–465.
- Pan X, Yang X, Lin G, Zou R, Chen H, Šamaj J and Xu C (2011) Ultrastructural changes and the distribution of arabinogalactan proteins during somatic embryogenesis of banana (Musa spp. AAA cv. 'Yueyoukang 1'). *Physiol Plant* **142**, 372–389.
- Wang X, Shi L, Lin G, Pan X, Chen H, Wu X, Takáč T, Šamaj J and Xu C (2013) A systematic comparison of embryogenic and non-embryogenic cells of banana (Musa spp. AAA): ultrastructural, biochemical and cell wall component analyses. *Sci Hortic* **159**, 178–185.
- Satoh S, Kamada H, Harada H and Fujii T (1986) Auxin-controlled glycoprotein release into the medium of embryogenic carrot cells. *Plant Physiol* **81**, 931–933.
- Fujimura T and Komamine A (1975) Effects of various growth regulators on the embryogenesis in a carrot cell suspension culture. *Plant Sci Lett* **5**, 359–364.
- Keller GL, Nikolau BJ, Ulrich TH and Wurtele ES (1988) Comparison of starch and ADP-glucose pyrophosphorylase levels in non-embryogenic cells and developing embryos from induced carrot cultures. *Plant Physiol* **86**, 451–456.
- Neves N, Segura-Nieto M, Blanco MA, Sánchez M, González A, González JI and Castillo R (2003) Biochemical characterization of embryogenic and non-embryogenic calluses of sugarcane. *In Vitro Cell Dev Biol Plant* **39**, 343–345.
- Mahmud I, Shrestha B, Boroujerdi A and Chowdhury K (2015) NMR-based metabolomics profile comparisons to distinguish between embryogenic and non-embryogenic callus tissue of sugarcane at the biochemical level. *In Vitro Cell Dev Biol Plant* **51**, 340–349.
- Jimenez VM and Bangerth F (2001) Endogenous hormone levels in explants and in embryogenic and non-embryogenic cultures of carrot. *Physiol Plant* **111**, 389–395.
- Jimenez VM and Bangerth F (2001) Hormonal status of maize initial explants and of the embryogenic and non-embryogenic callus cultures derived from them as related to morphogenesis *in vitro*. *Plant Sci* **160**, 247–257.
- Jimenez VM, Guevara E, Herrera J and Bangerth F (2005) Evolution of endogenous hormone concentration in embryogenic cultures of carrot during early expression of somatic embryogenesis. *Plant Cell Rep* **23**, 567–572.
- Martin AB, Cuadrado Y, Guerra H, Gallego P, Hita O, Martin L, Dorado A and Villalobos N (2000) Differences in the contents of total sugars, reducing sugars, starch and sucrose in embryogenic and non-

- embryogenic calli from *Medicago arborea* L. *Plant Sci* **154**, 143–151.
- 22 Moing A, Maucourt M, Renaud C, Gaudill Egrave, Re M, Brouquisse R, Lebouteiller B, Gousset-Dupont A, Vidal J, Granot D *et al.* (2004) Quantitative metabolic profiling by 1-dimensional <sup>1</sup>H-NMR analyses: application to plant genetics and functional genomics. *Funct Plant Biol* **31**, 889–902.
- 23 Mounet F, Lemaire-Chamley M, Maucourt M, Cabasson C, Giraudel J-L, Deborde C, Lessire R, Gallusci P, Bertrand A, Gaudillère M *et al.* (2007) Quantitative metabolic profiles of tomato flesh and seeds during fruit development: complementary analysis with ANN and PCA. *Metabolomics* **3**, 273–288.
- 24 Deborde C, Maucourt M, Baldet P, Bernillon S, Biais B, Talon G, Ferrand C, Jacob D, Ferry-Dumazet H, De Daruvar A *et al.* (2009) Proton NMR quantitative profiling for quality assessment of greenhouse-grown tomato fruit. *Metabolomics* **5**, 183–198.
- 25 Allwood JW, De Vos RC, Moing A, Deborde C, Erban A, Kopka J, Goodacre R and Hall RD (2011) Plant metabolomics and its potential for systems biology research background concepts, technology, and methodology. *Methods Enzymol* **500**, 299–336.
- 26 Hendriks JHM, Kolbe A, Gibon Y, Stitt M and Geigenberger P (2003) ADP-glucose pyrophosphorylase Is activated by posttranslational redox-modification in response to light and to sugars in leaves of *Arabidopsis* and other plant species. *Plant Physiol* **133**, 838–849.
- 27 Poompachee K and Chudapongse N (2012) Comparison of the antioxidant and cytotoxic activities of *Phyllanthus virgatus* and *Phyllanthus amarus* extracts. *Med Princ Pract* **21**, 24–29.
- 28 Nunes-Nesi A, Carrari F, Gibon Y, Sulpice R, Lytovchenko A, Fisahn J, Graham J, Ratcliffe RG, Sweetlove LJ and Fernie AR (2007) Deficiency of mitochondrial fumarase activity in tomato plants impairs photosynthesis via an effect on stomatal function. *Plant J* **50**, 1093–1106.
- 29 Gibon Y, Blaesing OE, Hannemann J, Carillo P, Höhne M, Hendriks JHM, Palacios N, Cross J, Selbig J and Stitt M (2004) A robot-based platform to measure multiple enzyme activities in *Arabidopsis* using a set of cycling assays: comparison of changes of enzyme activities and transcript levels during diurnal cycles and in prolonged darkness. *Plant Cell* **16**, 3304–3325.
- 30 Cross JM, Von Korff M, Altmann T, Bartzetko L, Sulpice R, Gibon Y, Palacios N and Stitt M (2006) Variation of enzyme activities and metabolite levels in 24 *Arabidopsis* accessions growing in carbon-limited conditions. *Plant Physiol* **142**, 1574–1588.
- 31 Biais B, Bénard C, Beauvoit B, Colombié S, Prodhomme D, Ménard G, Bernillon S, Gehl B, Gautier H, Ballias P *et al.* (2014) Remarkable reproducibility of enzyme activity profiles in tomato fruits grown under contrasting environments provides a roadmap for studies of fruit metabolism. *Plant Physiol* **164**, 1204–1221.
- 32 Manjunath S, Lee CH, Vanwinkle P and Bailey-Serres J (1998) Molecular and biochemical characterization of cytosolic phosphoglucomutase in maize. Expression during development and in response to oxygen deprivation. *Plant Physiol* **117**, 997–1006.
- 33 Huege J, Sulpice R, Gibon Y, Lisec J, Koehl K and Kopka J (2007) GC-EI-TOF-MS analysis of *in vivo* carbon-partitioning into soluble metabolite pools of higher plants by monitoring isotope dilution after <sup>13</sup>CO<sub>2</sub> labelling. *Phytochemistry* **68**, 2258–2272.
- 34 Piques M, Schulze WX, Hohne M, Usadel B, Gibon Y, Rohwer J and Stitt M (2009) Ribosome and transcript copy numbers, polysome occupancy and enzyme dynamics in *Arabidopsis*. *Mol Syst Biol* **5**, 314.
- 35 Rolin D, Deborde C, Maucourt M, Cabasson C, Fauvelle F, Jacob D, Canlet C and Moing A (2013) Chapter One: high-resolution <sup>1</sup>H-NMR spectroscopy and beyond to explore plant metabolome. In *Advances in Botanical Research* (Dominique R, ed), pp. 1–66. Academic Press, San Diego, CA.
- 36 Blanc G, Lardet L, Martin A, Jacob JL and Carron MP (2002) Differential carbohydrate metabolism conducts morphogenesis in embryogenic callus of *Hevea brasiliensis* (Mull. Arg.). *J Exp Bot* **53**, 1453–1462.
- 37 Sablowski R and Carnier Dornelas M (2014) Interplay between cell growth and cell cycle in plants. *J Exp Bot* **65**, 2703–2714.
- 38 Dante RA, Larkins BA and Sabelli PA (2014) Cell cycle control and seed development. *Front Plant Sci* **5**, 493. 1–14.
- 39 Collins C, Dewitte W and Murray JA (2012) D-type cyclins control cell division and developmental rate during *Arabidopsis* seed development. *J Exp Bot* **63**, 3571–3586.
- 40 Riou-Khamlichi C, Huntley R, Jacquard A and Murray JAH (1999) Cytokinin activation of *Arabidopsis* cell division through a D-Type Cyclin. *Science* **283**, 1541–1544.
- 41 Riou-Khamlichi C, Menges M, Healy JM and Murray JA (2000) Sugar control of the plant cell cycle: differential regulation of *Arabidopsis* D-type cyclin gene expression. *Mol Cell Biol* **20**, 4513–4521.
- 42 Hirano H, Harashima H, Shinmyo A and Sekine M (2008) *Arabidopsis* Retinoblastoma-Related Protein 1 is involved in G1 phase cell cycle arrest caused by sucrose starvation. *Plant Mol Biol* **66**, 259–275.
- 43 Menges M, De Jager SM, Gruissem W and Murray JA (2005) Global analysis of the core cell cycle regulators of *Arabidopsis* identifies novel genes, reveals multiple and highly specific profiles of expression and provides a

- coherent model for plant cell cycle control. *Plant J* **41**, 546–566.
- 44 Komaki S and Sugimoto K (2012) Control of the plant cell cycle by developmental and environmental cues. *Plant Cell Physiol* **53**, 953–964.
- 45 Schruff MC, Spielman M, Tiwari S, Adams S, Fenby N and Scott RJ (2006) The Auxin Response Factor 2 gene of Arabidopsis links auxin signalling, cell division, and the size of seeds and other organs. *Development* **133**, 251–261.
- 46 Ohto MA, Floyd SK, Fischer RL, Goldberg RB and Harada JJ (2009) Effects of *Apeta2* on embryo, endosperm, and seed coat development determine seed size in Arabidopsis. *Sex Plant Reprod* **22**, 277–289.
- 47 Dewitte W, Scofield S, Alcasabas AA, Maughan SC, Menges M, Braun N, Collins C, Nieuwland J, Prinsen E, Sundaresan V *et al.* (2007) Arabidopsis CYCD3 D-type cyclins link cell proliferation and endocycles and are rate-limiting for cytokinin responses. *Proc Natl Acad Sci USA* **104**, 14537–14542.
- 48 Yoshizumi T, Tsumoto Y, Takiguchi T, Nagata N, Yamamoto YY, Kawashima M, Ichikawa T, Nakazawa M, Yamamoto N and Matsui M (2006) Increased level of polyplody1, a conserved repressor of CYCLINA2 transcription, controls endoreduplication in Arabidopsis. *Plant Cell* **18**, 2452–2468.
- 49 Strickland SG, Nichol JW, McCall CM and Stuart DA (1987) Effect of carbohydrate source on alfalfa somatic embryogenesis. *Plant Sci* **48**, 113–121.
- 50 Batty N and Dunwell J (1989) Effect of maltose on the response of potato anthers in culture. *Plant Cell, Tissue Organ Cult* **18**, 221–226.
- 51 Orshinsky BR, Mcgregor LJ, Johnson GI, Hucl P and Kartha KK (1990) Improved embryoid induction and green shoot regeneration from wheat anthers cultured in medium with maltose. *Plant Cell Rep* **9**, 365–369.
- 52 Kunitake H, Nakashima T, Mori K and Tanaka M (1997) Normalization of asparagus somatic embryogenesis using a maltose-containing medium. *J Plant Physiol* **150**, 458–461.
- 53 Scott RL, Lyne AJ and Rees T (1995) Metabolism of maltose and sucrose by microspores isolated from barley (*Hordeum vulgare* L.). *Planta* **197**, 435–441.
- 54 Leegood RC, Labate CA, Huber SC, Neuhaus HE and Stitt M (1988) Phosphate sequestration by glycerol and its effects on photosynthetic carbon assimilation by leaves. *Planta* **176**, 117–126.
- 55 Brouquisse R, Rolin D, Cortes S, Gaudillere M, Evrard A and Roby C (2007) A metabolic study of the regulation of proteolysis by sugars in maize root tips: effects of glycerol and dihydroxyacetone. *Planta* **225**, 693–709.
- 56 Aubert S, Gout E, Bligny R, Marty-Mazars D, Barrieu F, Alabouvette J, Marty F and Douce R (1996) Ultrastructural and biochemical characterization of autophagy in higher plant cells subjected to carbon deprivation: control by the supply of mitochondria with respiratory substrates. *J Cell Biol* **133**, 1251–1263.
- 57 Vu JCV, Niedz RP and Yelenosky G (1993) Glycerol stimulation of chlorophyll synthesis, embryogenesis, and carboxylation and sucrose metabolism enzymes in nuclear callus of ‘Hamlin’ sweet orange. *Plant Cell, Tissue Organ Cult* **33**, 75–80.
- 58 Bellettre A, Couillerot J-P and Vasseur J (1999) Effects of glycerol on somatic embryogenesis in Cichorium leaves. *Plant Cell Rep* **19**, 26–31.
- 59 Diaz-Ruiz R, Rigoulet M and Devin A (2011) The Warburg and Crabtree effects: on the origin of cancer cell energy metabolism and of yeast glucose repression. *Biochim Biophys Acta* **1807**, 568–576.
- 60 Yu SM, Kuo YH, Sheu G, Sheu YJ and Liu LF (1991) Metabolic derepression of alpha-amylase gene expression in suspension-cultured cells of rice. *J Biol Chem* **266**, 21131–21137.
- 61 Miyazawa Y, Sakai A, Miyagishima S-Y, Takano H, Kawano S and Kuroiwa T (1999) Auxin and cytokinin have opposite effects on amyloplast development and the expression of starch synthesis genes in cultured Bright yellow-2 tobacco cells. *Plant Physiol* **121**, 461–470.

## Supporting information

Additional Supporting Information may be found online in the supporting information tab for this article:

**Fig. S1.** <sup>1</sup>H-NMR spectra of cellular metabolites. EC (red), NEC (black).

**Fig. S2.** <sup>1</sup>H-NMR spectra of metabolites in culture media. EC (red), NEC (black).